

4-2019

The Proliferation of Porcine Retinal Ganglion Cells Using PNU 282987

Rebecca Karl
Grand Valley State University

David Linn
Grand Valley State University

Follow this and additional works at: <https://scholarworks.gvsu.edu/honorsprojects>



Part of the [Eye Diseases Commons](#), and the [Ophthalmology Commons](#)

ScholarWorks Citation

Karl, Rebecca and Linn, David, "The Proliferation of Porcine Retinal Ganglion Cells Using PNU 282987" (2019). *Honors Projects*. 738.
<https://scholarworks.gvsu.edu/honorsprojects/738>

This Open Access is brought to you for free and open access by the Undergraduate Research and Creative Practice at ScholarWorks@GVSU. It has been accepted for inclusion in Honors Projects by an authorized administrator of ScholarWorks@GVSU. For more information, please contact scholarworks@gvsu.edu.

The Proliferation of Porcine Retinal Ganglion Cells Using PNU 282987

Rebecca Karl and Dr. David Linn of the Biomedical Sciences Department
of
Grand Valley State University

For the fulfillment of the Honors Senior Project of the Frederick Meijer Honors College

April 2019

Abstract

The retinal ganglion cells (RGCs) from porcine eyes were extracted to work towards a potential therapy for glaucoma. There is not a known cause of glaucoma or the apoptosis of RGCs that cause the eventual blindness associated with glaucoma. The goal of this protocol is to protect the RGCs from dying by adding a nicotinic acetylcholine receptor activator to induce neuronal proliferation and protect against glutamate-induced excitotoxicity. PNU 282987 was used as the nicotinic acetylcholine receptor activator due to its neuroprotective properties. We hypothesized that we would observe the proliferation of RGCs (associated with increased cell numbers) with varying levels of PNU 282987 compared to a set of untreated control plates. For each protocol three plates labelled A were left untreated, three plates labelled B were treated with 40 μ L of PNU 282987 (100 μ M), and three plates labelled C were treated with 80 μ L of PNU 282987 (200 μ M). We analyzed pictures of the plates using Image J. The average cell count and average area were analyzed for our purposes to check for the proliferation of RGCs and determine the size of the cells that survived and replicated. Although there seemed to be an increased average cell count in plates B compared to plates A and C and an increase in average area in plates C compared to plates A and B, our data did not have statistical significance. Further experiments will have to be conducted to determine if PNU 282987 significantly induces the proliferation of RGCs, and if its neuroprotective properties can be used as a potential treatment for glaucoma or provide further insight into the cause of this disease.

Introduction

Glaucoma is an ocular neurodegenerative disease that is caused by the death of retinal ganglion cells (RGCs) and their axons which eventually leads to blindness.¹⁻⁶ RGCs interact indirectly with the photoreceptors that receive the light that enters the eye. RGCs, whose axons form the optic nerve, transmits the image to our brain to be interpreted. These RGCs die via apoptosis presumably due to glutamate-induced excitotoxicity.³⁻⁷ Müller glia cells usually are responsible for protecting neurons such as RGCs against glutamate-induced excitotoxicity by clearing glutamate.^{8,9} Many have believed that an increase in intraocular pressure (IOP) is a cause of glaucoma, yet there are patients with normotensive (normal IOP) glaucoma. But there seems to be strong correlation between a high IOP and the degeneration of RGCs. If one already has glaucoma, an increased IOP has been correlated with faster development of glaucoma.² An elevated IOP has been shown to be followed by a decrease in mitochondria in the optic nerve.^{10,11} It can be unsafe to alter a patient's blood pressure in order to attempt to lower the IOP², so other treatment options for glaucoma such as directly addressing the death of RGCs may be a safer and more effective option for patients.

Large RGCs seem to be targeted especially during apoptosis, but RGCs of all sizes are affected by this disease.⁵ The death of the axons negatively affects vision due to the loss of transportation of substances between the cell body and axon terminal. This could cause the RGCs to die due to an intracellular electrolyte imbalance or microglial phagocytosis.¹²

RGC regeneration has been seen in other organisms, for example the zebrafish.^{13,14} Once the RGCs have sustained damage, Müller glia are induced to dedifferentiate into multipotent neural progenitor cells.^{8,9} These cells move to the damaged region of the retina and differentiate into the cell type that was damaged.¹⁴ Due to the successful regeneration of

retinal cells in other organisms, we believe that this line of research can be extended to mammalian retinas, specifically porcine retinas. It has been shown that insulin growth factor inhibitors can halt the proliferation of certain tissues.¹⁴ In order to combat this, we enrich the second media with insulin, transferrin and nerve-growth factor. Importantly, a recent study has shown that Müller glia are involved in the proliferation of RGCs in rodent retinas in response to alpha7 nicotinic acetylcholine receptors (nAChR) agonists.^{15,16}

Mammalian nervous systems have an abundance of nicotinic receptors for acetylcholine.¹⁷ For this protocol, we focused on targeting the nAChR found near the optic nerve because there is evidence to show that these receptors are neuroprotective.^{1,3,4,6,18} But, a recent study in a rodent model of glaucoma, provided evidence for the role of retinal pigment epithelium (RPE) of responding to such compounds and inducing proliferation from Müller glia.^{15,16} Most research on glaucoma has focused on the issue of IOP within the eye. IOP is not always a consistent indicator of glaucoma or its severity, and even if the IOP is treated, oftentimes RGCs continue to die.¹⁹ To get to the root of the problem of this disease, we have attempted to induce proliferation of RGCs in a mixed retinal cell culture using PNU 282987. PNU 282987 has been shown to have neuroprotective properties on isolated RGCs³, so we hypothesize that PNU 282987 will protect existing RGCs and possibly cause a proliferation of RGCs in culture and an increase in average size and numbers due to mitosis taking place.

Methods

Sterile Technique

The timeline for the experiment is shown in Figure 1. The porcine eyes were obtained from DeVries Meats in Coopersville, MI. The sterile technique begins by wiping down the hood with ~40% ethanol solution. Then place the 1000 µL pipette and pipette tips; the 200 µL pipette and pipette tips; small plastic autoclaved vials; a white-capped glass vial; Parafilm; scissors; tape; Kimwipes; Sharpie; automatic pipette and two disposable plastic

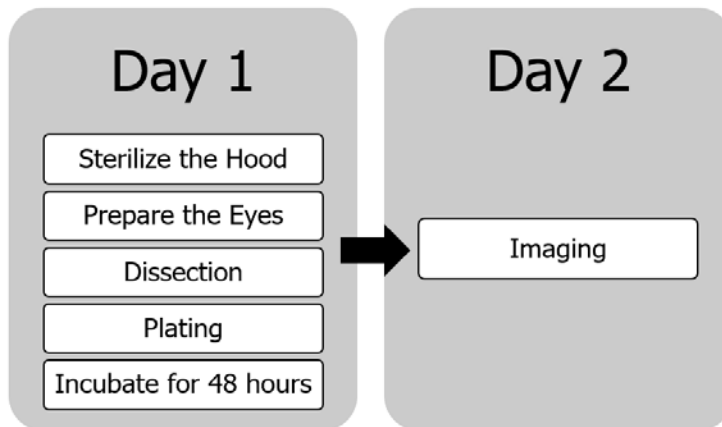


Figure 1: Experimental Timeline. On the first day of the protocol, one must sterilize the hood, clean the eyes by removing the flesh around the eye and ocular nerve, dissect the eyes, plate the cells and incubate the plates for 48 hours. After the 48 hours, take pictures of each of the plates.

pipette tips; autoclaved glass pipette tips and pipette bulb; Fischer plates; 100 mL beaker; dissecting scissors; scalpel, and forceps in the hood. Turn the UV light and the blower on with the hood slightly open for 20 minutes. Be sure to wear gloves and sterilize the gloves with ethanol each time you enter the hood.

Preparing the Eyes

Remove the DNase, insulin (10 mg/mL), transferrin (500 µg/mL) and nerve growth factor from the freezer to thaw. Label two 50 mL plastic centrifuge tubes Media #1 and Media #2. Fill Media #1 with 33 mL and Media #2 with 36 mL of CO₂-Independent Medium. Add 3.5 mL of pig ringers solution to the white capped glass vial. Combine 87.5 µL of papain with 210 µL of papain activating solution in a small autoclaved plastic vial. Incubate the vial while dissecting. Dissect 6 retinas per protocol. First, remove the flesh around each eye using the dissecting scissors while at the lab bench. Place the eyes in a 100 mL beaker with ice. Move to the hood for the remainder of the dissection. Turn off the UV light and blower when dissecting.

Dissection

Use a Fischer plate to dissect the eyes, the bottom with the taller lip for dissecting, and the top for isolating the RGCs once they have been extracted. To dissect an eye, take the scalpel and make an incision about eight centimeters away from the iris. Gently push the eye up against the lip of the dish for stability. Be sure to not place too much pressure on the eye. Once the incision has been made, take the forceps and grasp the eye and use the dissecting scissors to continue the incision around the iris until the anterior and posterior parts of the eye are separated. Now take another set of forceps in place of the dissecting scissors and use these to remove the thin layer of opaque RGCs from the back of the eye. Avoid extracting the black retinal pigmented epithelium (RPE) with the RGCs. Place the RGCs in the adjacent dish, and using the scalpel, chop up the RGCs. Transfer the RGCs to the white capped glass vial. Clean the dishes with ethanol and wipe with Kimwipes. Repeat this process for the remaining eyes.

Add the vial of papain and papain activating solution to the white capped vial and incubate for 20 minutes at 37°C, shaking every 7 minutes. During incubation, label nine Fischer plates using the Sharpie: A1, A2, A3, B1, B2, B3, C1, C2, and C3 as shown in Figure 2. Write

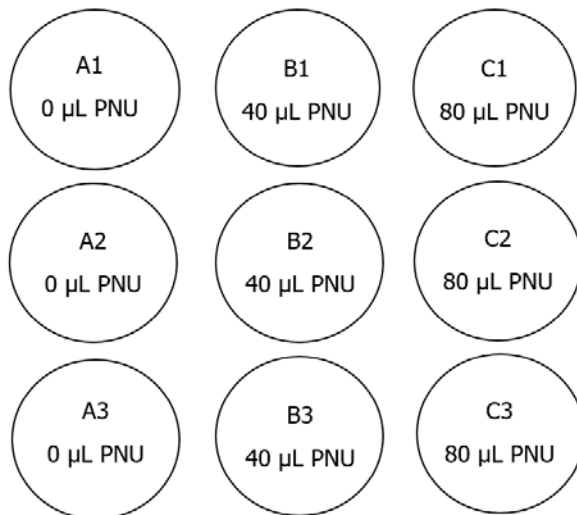


Figure 2: Fischer Plate Setup. The plates were labelled A1-C3. The plates labelled A received no PNU 282987 and were used as a control. The plates labelled B were given 40 µL of PNU 282987. The plates labelled C were given 80 µL of PNU 282987.

initials and date of the experiment on each plate with the number one on it. Enrich Media #2 with 75 µL of nerve growth factor, 72 µL of transferrin, and 18 µL of insulin using a 200 µL pipette.

Plating and Incubation

After incubation, return to the hood with the white capped glass vial and add 100 μL of DNase. Let sit for one minute. Take the glass pipette tip and begin to transfer the retina mixture from the white-capped glass vial to the Media #1 tube. As you go, filter blood vessels and black RPE cells out on to a paper towel. Once the filtered retina mixture has been added to Media #1, shake Media #1 well, and using the automatic pipette to add 3 mL of the mixture to each of the nine Fischer plates that are labelled. Be sure that the bottom of the plates are coated evenly. Place them in the incubator at 37°C for one hour. Remove all excess equipment from the hood except for the automatic pipette, Kimwipes, parafilm, 200 μL pipette and pipette tips. Place the vacuum flask, its attachments, a glass pipette tip and a clean 100 mL beaker inside the hood. Turn on the UV light and the blower on with the hood slightly open to disinfect the hood. Remove the PNU 282987 from the fridge to thaw.

Remove the plates after one hour and return them to the hood. Use the vacuum to remove the media from the plates. Fill the 100 mL with a small amount of ethanol. Dip the tip of the pipette in ethanol. Gently tip each plate on an angle and touching the tip of the pipette to the wall of the plate, not the bottom. Between each plate, dip the pipette in ethanol to disinfect. Add 4 mL of Media #2 to each Fischer plate. Be sure that the bottom of the plates are coated evenly as before.

The plates labelled A are the control. Add nothing to them. Add 40 μL of the PNU 282987 to the B plates. Add 80 μL of the PNU 282987 to the C plates. Cover the plates and place them in the incubator for 48 hours at 37°C.

Imaging

Remove the plates from the incubator. Use the Nikon Eclipse E400 to image the cells. Use the DAPI setting and the 10x magnification on the microscope. Wait for the cells to settle and stop moving before you capture an image. Take one picture of each plate and label them as they are labelled on the Fischer plates, A1-C3. Save them separately to a flash drive for analysis. Use Image J to analyze the images of the plates. We used Image J to count the cells and determine their average size in μm^2 .

Results

The two variables measured from the images taken were the average number of cells in the picture of each plate and the average area of the cells. Examples of these images from each plate are shown below in Figure 3. The cells were counted using a threshold technique to contrast from the background.

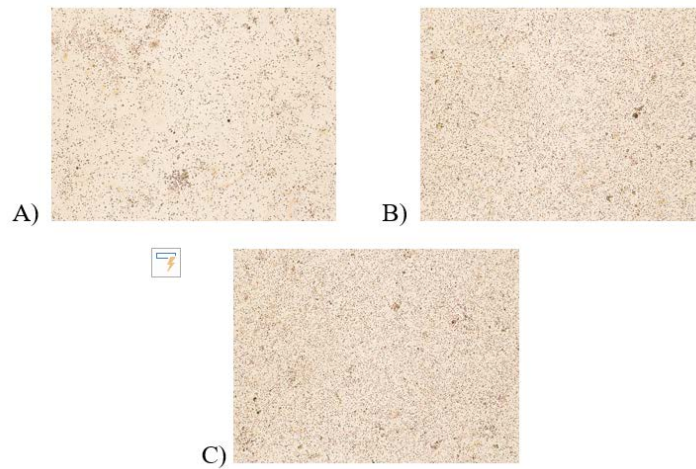


Figure 3: Pictures of Plates A, B and C. (A) This is a sample of an image taken of an A plate. The cells are shown against the beige background. (B) This shows an example of an image of the cells found on a B plate. (C) This image shows the cells found on a C plate.

The A plates, the control, had an average of 1908.4 cells per picture with a standard error of the mean of 447.125. The B plates, treated with 40 μL of PNU, had an average of 2280.095 cells per picture with a standard error of the mean of 639.98. The C plates, treated with 80 μL of PNU, had an average of 1844.95 cells per picture with a standard error of the mean 623.367. These values are shown in Figure 4. There appears to be an increase in cell numbers in the B plates compared to the A plates and C plates.

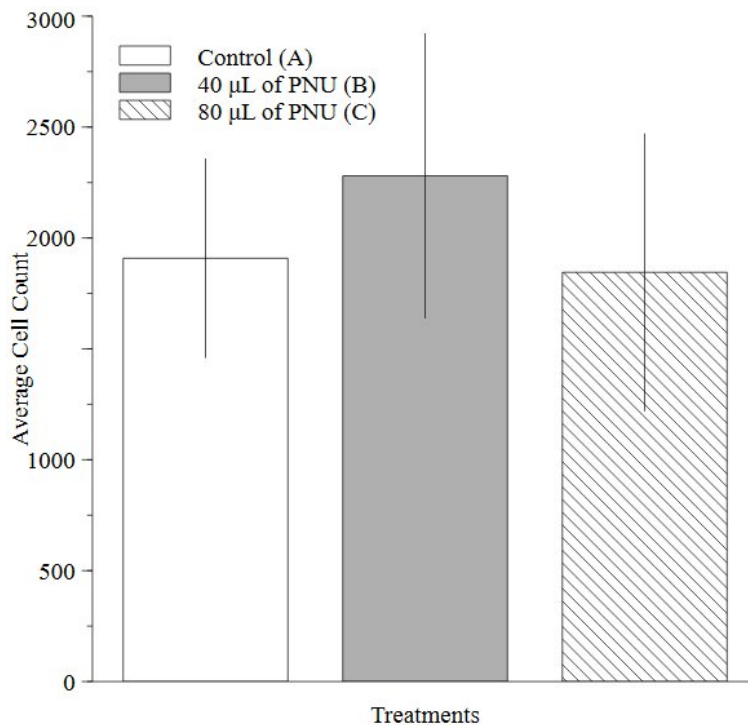


Figure 4: Average Cell Count. The A plates (control) had an average of 1908.4 cells per picture with a standard error of the mean (SEM) of 447.125. The B plates (40 μL of PNU 282987) had an average of 2280.095 cells per picture with an SEM of 639.98. The C plates (80 μL of PNU 282987) had an average of 1844.95 cells per picture and an SEM of 623.367.

The C plates had the largest average area of a cell of $362,552 \mu\text{m}^2$ with a standard error of the mean of $158,887.7$. Plates A and B have similar average area. The average area of the A plates is $191,241.8 \mu\text{m}^2$ with a standard error of the mean of $120,262$. The average area of the B plates is $181,194.9 \mu\text{m}^2$ with a standard error of the mean of $115,988.4$. These values can be seen in Figure 5. Although the B plates appear to have the largest average area of its cells when comparing the three plates, there was no statistical significance with this data set, so we cannot say that there is a difference among the three variables.

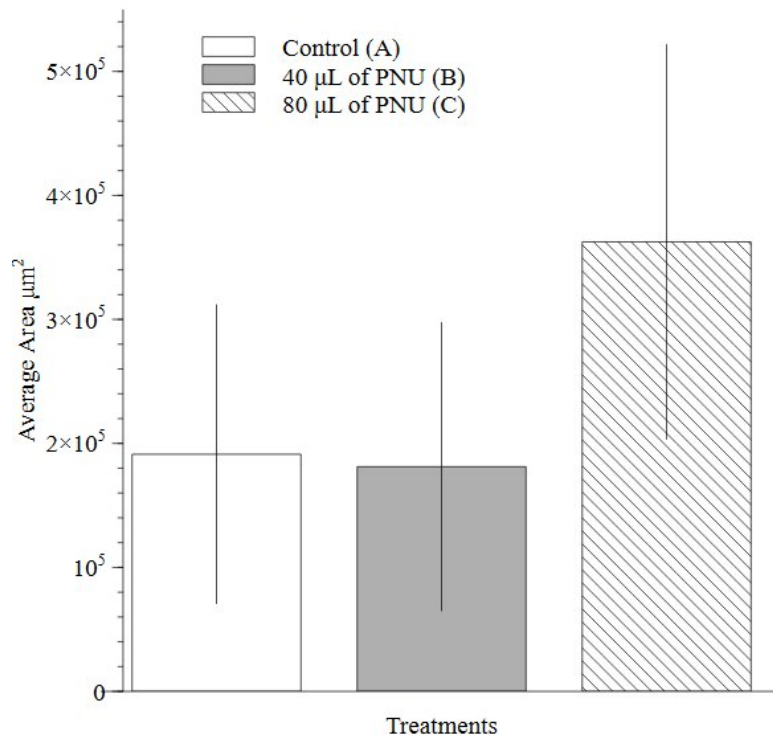


Figure 5: Average Area. The average area that the cells take up in the pictures of the A plates is $191,241.8 \mu\text{m}^2$ with a SEM of $120,262$. The average area that the cells take up in the pictures of the B plates is $181,194.9 \mu\text{m}^2$ with a SEM of $115,988.4$. The average area that the cells take up in the pictures of plates C is $362,552 \mu\text{m}^2$ with a SEM of $158,887.7$.

Discussion

The described protocol was run seven times. We compared the average cell count between the plates to determine if mitosis had occurred since there should be more cells if proliferation had occurred. A cellular count that is significantly higher or lower in any of the plates would tell us if PNU 282987 was effective at stimulating mitosis in RGCs. Although it appeared that the B plates treated with $40 \mu\text{L}$ ($100 \mu\text{M}$) of PNU 282987 did have an increase in the cell count, Figure 3 shows that the cumulative data surrounding cell count was statistically insignificant. We may have seen an increase in cell count in only the B plates because $80 \mu\text{L}$ ($200 \mu\text{M}$) of PNU 282987 may have surpassed the saturation point of the RGCs rendering the excess PNU detrimental to the RGCs. Or, the higher dose was not the optimal dose to see an effect after the time we cultured our cells. $100 \mu\text{M}$ was found to be most effective over a comparable time frame when examining isolated RGCs in culture.²⁰

We compared the average cell size because a change in cell size could be considered as potential proof of cells going through replication and thus mitotic division. The average

diameter of a RGC is between 7 and 21.5 μm^{21} making the range of the average area of a RGC between 153.94 μm^2 and 1452.2 μm^2 . However, it appears in Figure 4 that the C plates (200 μM) had the largest cells according to the average area of 362,552 μm^2 . This could indicate that mitosis was indeed occurring in the RGCs since the cells were larger compared to the A and B plates as well as the average area of RGCs. The average cell size found on the C plates (200 μM) were almost twice as large as the RGCs on the control plates. Although the average area we observed for the control plates, 191,241.8 μm^2 , does not fit within the expected range of the average area of an RGC, we would expect that the proper amount of PNU 282987 would double the size of those cells due to the replication of those existing cells.

Even though the C plates had a lower average cell count as shown in Figure 3, that could have occurred because the cells that were amid replication had not divided yet. However, since this data was also statistically insignificant, more data would have to be collected to support this hypothesis. Conversely, one might expect the average cell size to be smaller after this relatively short incubation time since it would take time for cells to grow to full size.

Limitations

Human error needs to be considered a limitation during data collection. There are four students in the lab, and not all the protocols were done by the same student. For everyone to get experience using the microscope, the pictures were taken by different people within the lab. If the number of data sets had been larger, this too would have given us more accurate data since an increased sample size reduces random error. Due to time constraints and technical issues, only seven protocols were able to be completed for this paper.

When the plates were filled, the Media #1 was shaken, then promptly filled the plates starting with plate A1 every time. Even though the media was shaken prior to each plate being filled, we cannot guarantee that an equal amount of RGCs were distributed among the nine plates. My hypothesis is that since the A plates were filled first, they received the most RGCs. Even if there were proliferation in the plates labelled B and C, if all plates did not start out with close to equal number of cells, then we cannot be sure that proliferation took place or if the PNU 282987 was effective in any way. In future protocols I would suggest that we start by filling plates B or C and then rotate to eliminate or diminish this confounding variable. However, this was explored with isolated RGCs, and with enough shaking, no significant difference was found using different plating routines. But one cannot rule out that this mixed retinal cell system would be different.

Only one picture was taken of each plate and that could lead to an inaccurate representation of the total amount of cells on each plate. The visual field of the microscope could not cover the entire area of the plate, so we cannot be sure that the pictures taken of the plates were an accurate representation of the cell counts on each plate. To diminish the effect of this confounding variable, next time I would take multiple pictures of each plate. I would take at least four pictures of each plate by turning the plate ninety degrees for each picture taken. This is the usual protocol for the isolated RGC culture system, with images captured at 'north, south, east and west'.

Since the cells were plated in a liquid media, they did not have the chance to adhere to the bottom of the plate; they were suspended in the liquid. This allowed the cells to move about freely when the plates were moved. This could have posed problems in the following ways. When replacing Media #1 with the enriched Media #2, cells could have been removed

due to the vacuum. This could have resulted in a lower cell count in certain plates. When imaging, the cells had to take time to settle and stop their movement within the media. We had no control over the distribution of the cells in the plates. This could have resulted in the images not accurately representing the typical concentration of cells throughout the entire plate. However, with isolated RGC cultures, it was observed that cells that adhered to the surface were more viable and floating cells were usually dead or dying.

Moving forward, we would check the circularity of the cells to ensure that we are observing RGCs. A rating of 1 means that the cell is perfectly circular, and as the rating approaches zero, the cell become more elliptical.²² This would function as a confirmation of the specific cell type we have been observing. We would also increase the magnification of the Nikon Eclipse E400 by one degree of magnification, to the 40x magnification, in order to improve our counting of the cells and better analyze why some cells are larger than others, for example if some cells are proceeding through mitosis or not. These are issues with this relatively new mixed culture system and should benefit future experiments.

Conclusion

From the protocols run, we were unable to statistically determine if PNU 282987 was successful in targeting the $\alpha 7$ nicotinic acetylcholine receptors and activating their neuroprotective and proliferative properties. Due to the appearance of the data, we believe that there is the potential for PNU 282987 to be preventative in the progression of glaucoma as an effective activator of the nicotinic acetylcholine receptor and protector of RGCs. The appropriate amount of PNU 282987 has yet to be determined to reflect results observed in live rodents with experimentally induced glaucoma.¹⁵ The lab will continue to pursue potential treatments for glaucoma by focusing on the direct causes of blindness such as the death of RGCs rather than other symptoms such as increased IOP.

Literature Cited

1. Wehrwein, E., Thompson, S. A., Coulibaly, S. F., Linn, D. M. & Linn, C. L. Acetylcholine Protection of Adult Pig Retinal Ganglion Cells from Glutamate-Induced Excitotoxicity. *Invest. Ophthalmol. Vis. Sci.* **45**, 1531–1543 (2004).
2. Caprioli, J. & Coleman, A. L. Blood Pressure, Perfusion Pressure, and Glaucoma. *Am. J. Ophthalmol.* **149**, 704–712 (2010).
3. Iwamoto, K. *et al.* A Nicotinic Acetylcholine Receptor Agonist Prevents Loss of Retinal Ganglion Cells in a Glaucoma Model. *Investig. Ophthalmology Vis. Sci.* **55**, 1078 (2014).
4. Brandt, S. K., Weatherly, M. E., Ware, L., Linn, D. M. & Linn, C. L. Calcium preconditioning triggers neuroprotection in retinal ganglion cells. *Neuroscience* **172**, 387–397 (2011).
5. Quigley, H. A. Neuronal death in glaucoma. *Prog. Retin. Eye Res.* **18**, 39–57 (1999).
6. Thompson, S. A., Smith, O., Linn, D. M. & Linn, C. L. Acetylcholine neuroprotection against glutamate-induced excitotoxicity in adult pig retinal ganglion cells is partially mediated through $\alpha 4$ nAChRs. *Exp. Eye Res.* **83**, 1135–1145 (2006).
7. Garcia-Valenzuela, E., Shareef, S., Walsh, J. & Sharma, S. C. Programmed cell death of retinal ganglion cells during experimental glaucoma. *Exp. Eye Res.* **61**, 33–44 (1995).
8. Glial cells of the Retina by Helga Kolb – Webvision.
9. Reichenbach, A. & Robinson, S. R. The involvement of Müller cells in the outer retina. in *Neurobiology and Clinical Aspects of the Outer Retina* (eds. Djamgoz, M. B. A., Archer, S. N. & Vallergera, S.) 395–416 (Springer Netherlands, 1995). doi:10.1007/978-94-011-0533-0_16
10. Munemasa, Y., Kitaoka, Y., Kuribayashi, J. & Ueno, S. Modulation of mitochondria in the axon and soma of retinal ganglion cells in a rat glaucoma model. *J. Neurochem.* **115**, 1508–1519 (2010).
11. Kitaoka, Y. *et al.* Axonal protection by Nmnat3 overexpression with involvement of autophagy in optic nerve degeneration. *Cell Death Dis.* **4**, e860 (2013).
12. Thanos, S. Factors Retards Axotomy-induced Neuronal Degradation and Enhances Axonal Regeneration in viva and in vitro. *J. Neurosci.* **12**
13. Sherpa, T. *et al.* Ganglion cell regeneration following whole-retina destruction in zebrafish. *Dev. Neurobiol.* **68**, 166–181 (2008).
14. Gemberling, M., Bailey, T. J., Hyde, D. R. & Poss, K. D. The zebrafish as a model for complex tissue regeneration. *Trends Genet.* **29**, 611–620 (2013).
15. Webster, M. K. *et al.* Stimulation of Retinal Pigment Epithelium With an $\alpha 7$ nAChR Agonist Leads to Müller Glia Dependent Neurogenesis in the Adult Mammalian Retina. *Investig. Ophthalmology Vis. Sci.* **60**, 570 (2019).
16. Webster, M. K. *et al.* Evidence of BrdU-positive retinal neurons after application of an Alpha7 nicotinic acetylcholine receptor agonist. *Neuroscience* **346**, 437–446 (2017).
17. Albuquerque, E. X., Pereira, E. F. R., Alkondon, M. & Rogers, S. W. Mammalian Nicotinic Acetylcholine Receptors: From Structure to Function. *Physiol. Rev.* **89**, 73–120 (2009).
18. Oz, M., E. Lorke, D., S. Yang, K.-H. & Petroianu, G. On the Interaction of β -Amyloid Peptides and $\alpha 7$ -Nicotinic Acetylcholine Receptors in Alzheimer's Disease. (2013). Available at:

<https://www.ingentaconnect.com/content/ben/car/2013/00000010/00000006/art00007>.
(Accessed: 28th March 2019)

19. Linn, C. L. Retinal ganglion cell neuroprotection induced by activation of alpha7 nicotinic acetylcholine receptors. *Neural Regen. Res.* **11**, 918–919 (2016).
20. Lyons, L. NEUROPROTECTIVE EFFECT OF AN α -7 NICOTINIC ACETYLCHOLINE RECEPTOR AGONIST AND A POSITIVE ALLOSTERIC MODULATOR IN AN IN VITRO MODEL OF GLAUCOMA. (Grand Valley State University, 2014).
21. Danias, J. *et al.* Cytoarchitecture of the retinal ganglion cells in the rat. *Invest. Ophthalmol. Vis. Sci.* **43**, 587–594 (2002).
22. Ferreira, T. & Rasband, W. ImageJ User Guide. 198